Los Alamos
NATIONAL LABORATORY
memorandum

Los Alamos Neutron Science Center, LANSCE-1
Accelerator Physics and Engineering Group

To/MS: Distribution
From/MS: H. Takeda, LANSCE-1, H817
Phone/Fax: 5-0820/5-2904
Symbol: LANSCE-1:99-118
Date: June 4, 1999
Email: htakeda@lanl.gov

DESIGN EXERCISE OF SNS LINAC CONSISTING OF DTL AND CCL

1. Abstract

As a simplified approach to design a linac for the SNS, we consider a DTL and CCL combination of linac which accelerates an H^- beam from 402.5 MHz RFQ at 2.5 MeV to 100 MeV by a DTL and followed by a CCL which accelerates up to 1000 MeV. We assume a beam peak current 56 mA in our design. The rf frequency triples from 402.5 MHz DTL to the 1207.5 MHz CCL. The CCL segment has 14 cavities, and the drift space between the segments is $2\beta\lambda$. The DTL and CCL are connected with a quadrupole with appropriate drift space in between.

The DTL assumes a FFDD lattice, and the CCL assumes a FODO lattice. In this memo, we present the linac design, the general beam dynamics behavior with and without rf amplitude, rf phase errors, and the quadrupole errors which include misalignments.

2. Linac Design

(A). Beam matching procedure between DTL and CCL

As a first step, we calculate the zero current phase advances at the exit of DTL using the Trace3D code. To calculate the phase advance, we choose one transverse period FFDD near the exit of DTL. Figure 1. shows the matched zero current beam starting at 96.7 MeV. The zero current phase advances are $\sigma_0x = 53.7°$ $\sigma_0y = 54.7°$ $\sigma_0z = 22.2°$.

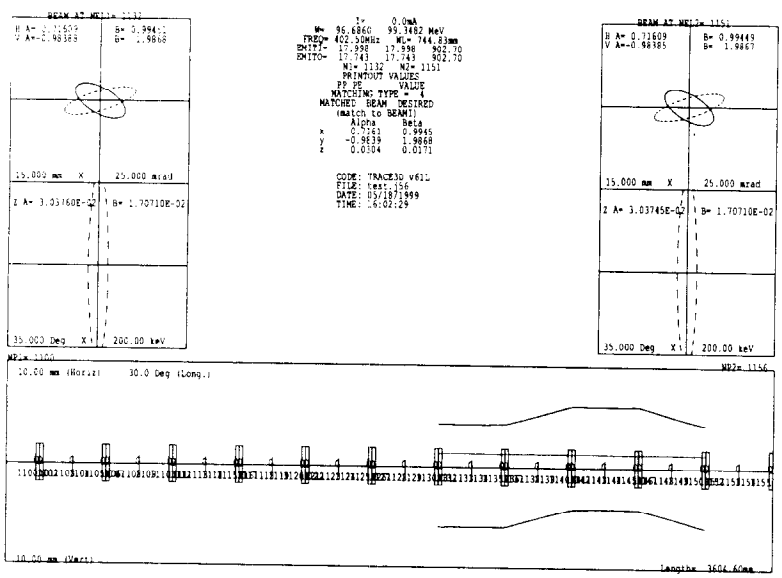

Fig. 1 The phase advance calculation for the zero current matched beam at the exit of DTL.

The CCL is designed as having a transverse period 18βλ with an operating frequency 1207.5 MHz. When a machining between different linac structure is performed such that the zero current phase advances in both longitudinal and transverse are made continuous, the beam will be matched regardless of the current without adjusting the linac(current independence). This continuity of zero current phase advance per unit length at the junction between 402.5 MHz DTL and CCL requires the zero current phase advances per period at the entry to the CCL as $\sigma x = 80.55°$ $\sigma y = 82.05°$ $\sigma z = 33.3°$.

To perform a beam matching from DTL to CCL, we need at least two independent bunching cavities and four quadrupoles. We choose the matching cavities as the first two segments of CCL and the matching quadrupoles as the three quads after each of the first three segments and a quadrupole between the DTL and the CCL. To satisfy the phase advance continuity condition, we need the following quadrupole strengths and accelerating gradients at the matching sections of CCL: the required quadrupole strengths are: -2.69718T (33.716G/cm x 8 cm), 2.235T (2794G/cm x 8 cm), -2.333T(2916.86 G/cm x 8 cm), 2.2334T (2791.8 G/cm x 8 cm). The first two segments of CCL each of which consisting 14 cavities is set to -90°. The RF amplitude of the two segments are set to 0.4748 MV/m and 0.4863MV/m respectively. They act as two sets of bunchers. Between the DTL and the CCL, after the protruding quadrupole of DTL, we have a drift space 38 cm followed by a quddrupole (2.69718T).

The beam envelopes at the matched state between DTL and the CCL as a result from Trace3D calculation is shown in Figure 2

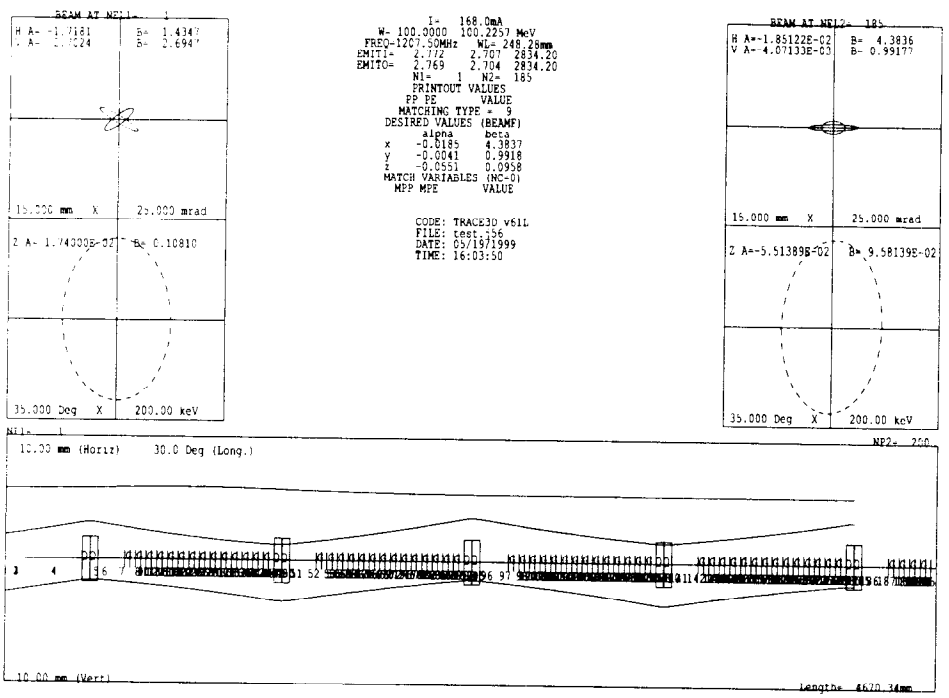

Figure 2. The matched beam envelope and the matching section of CCL at the entry. The preceding quadrupole to the CCL and the proceeding 3 quadrupoles are used for the transverse matching. The first two segments are operated at -90° to work as two bunchers.

(B) The designed linac parameters.

The linac accelerating field and design phase for the DTL and CCL are shown in figure 3 and 4 respectively. At the entry to the CCL, the E0 is required to be as low as 0.28 MV/m to satisfy the continuity of zero current phase advance per unit length. It is ramped rapidly to 3.74 MV/m. The DTL was designed by G. Neuschaffer. This DTL ramps the phase starting at -45° ramped to -25° at the first 48 cells (9.45 MeV). Then, stays constant up to 100 MeV. The CCL starts at the matching section with -50° and ramps rapidly to -24° at 117.7 MeV. Then the design phase stays constant. Total length of linac including the DTL is 475 m.

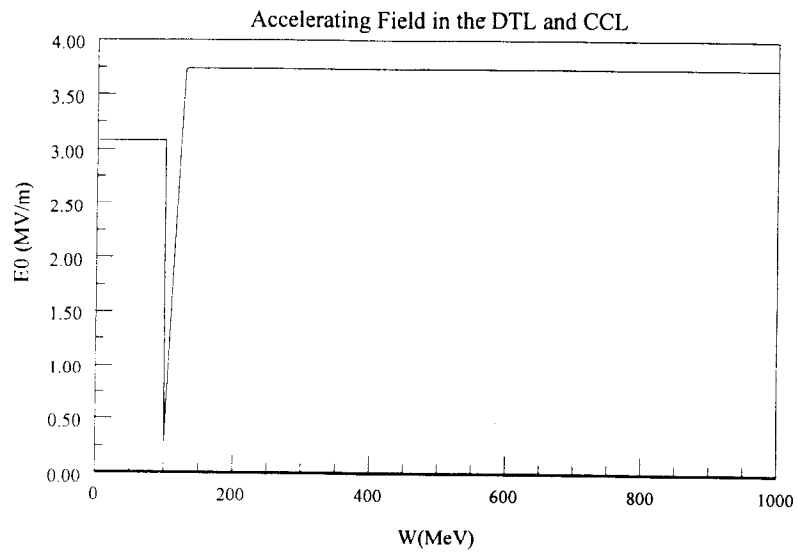

Fig. 3. Accelerating Cavity Field along the DTL and CCL.

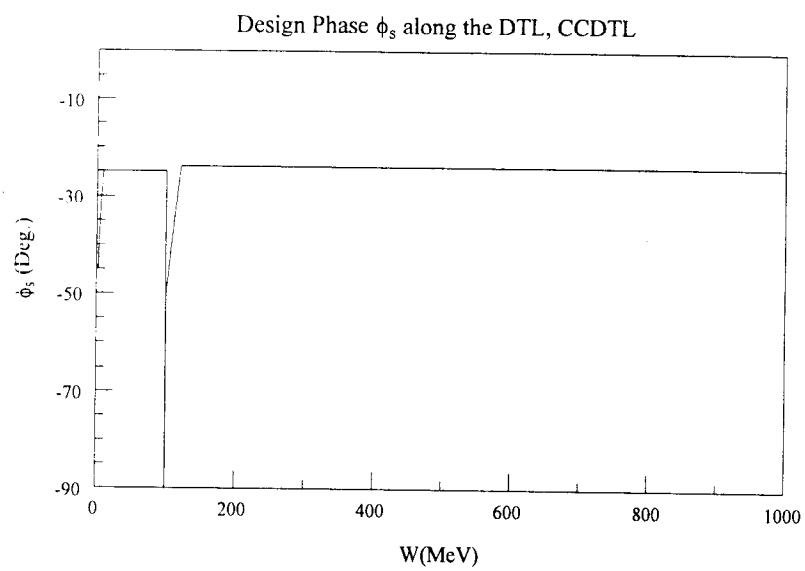

Fig. 4. Design phase along the DTL and CCL.

The quadrupole Gl product is chosen constant along the linac in the CCL. The Gl product is shown in Figure 5.

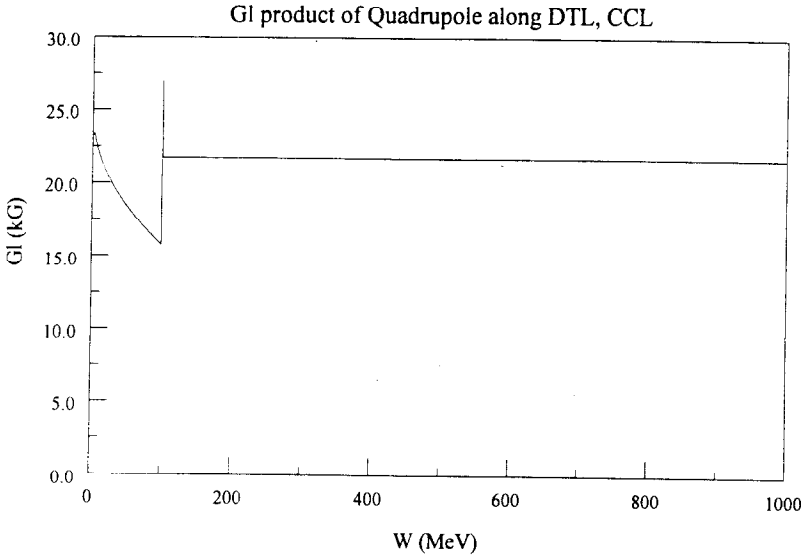

Fig. 5. Gl product of DTL and CCL along the Linac. The quadrupole Gl product was adjusted between DTL and CCL for the matching at 100 MeV.

3. Beam Dynamics Calculations

We inject a beam at 2.5 MeV into the DTL. The injected beam normalized rms emittances from the MEBT are εx=0.02012πcm-mr, εy=0.02429πcm-mr, and ε z=0.14194 deg-MeV.

(A) The beam dynamics calculation without errors

The beam profiles x, y, phase and energy along the entire linac are shown in Figure 6. Figure 7 shows the maximum and minimum beam sizes and the rms maximum and minimum sizes.

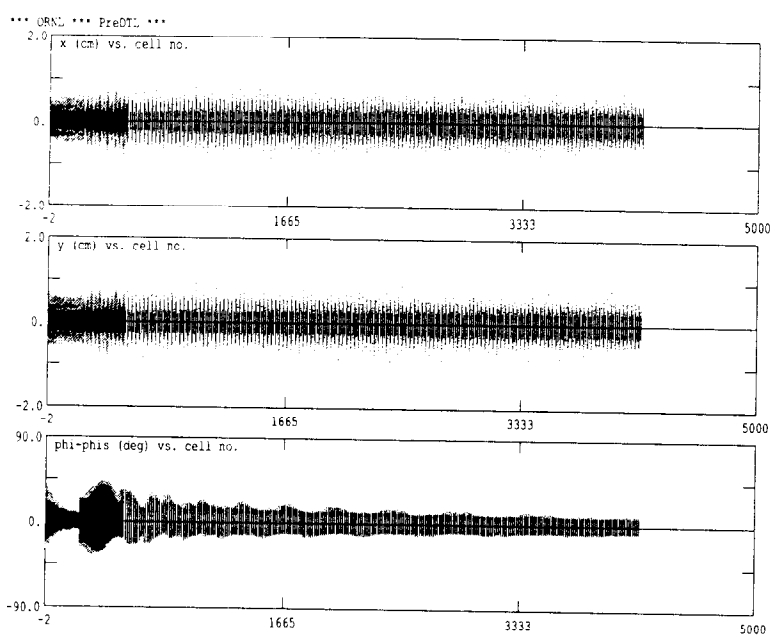

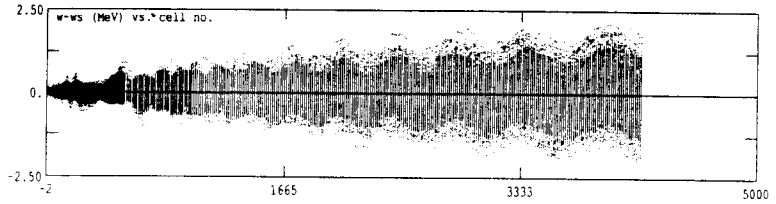

Fig. 6. The ideal beam envelope along the DTL and CCL. The rf phase, amplitude, and the quadrupoles have no errors.

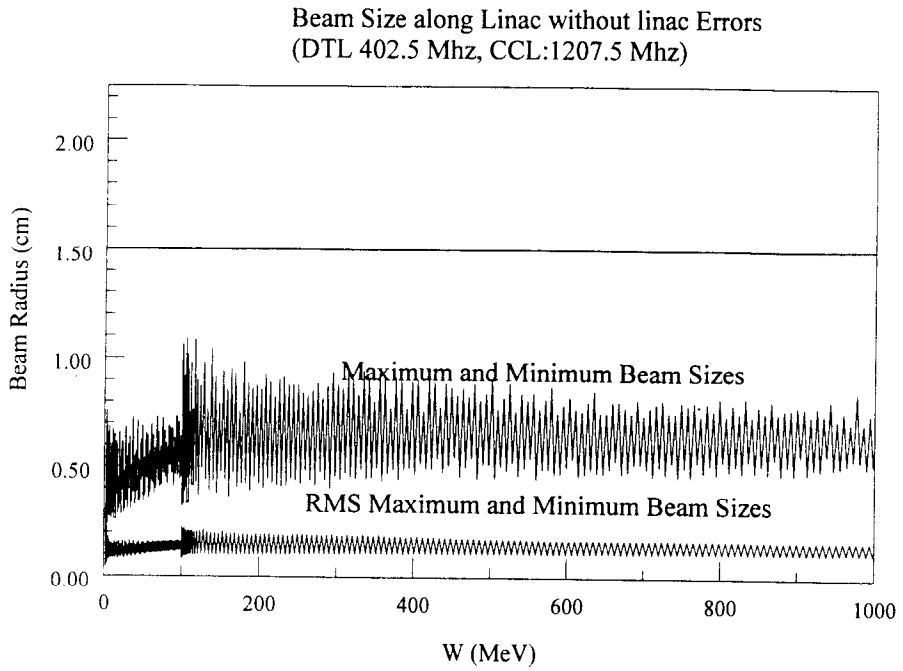

Fig. 7 Maximum and Minimum Beam Sizes (The beam has a maximum radius at focusing quadrupoles, and a minimum radius at defocusing quadrupoles in the FODO lattice). The RMS beam sizes are also shown from DTL entry to the end of CCL.

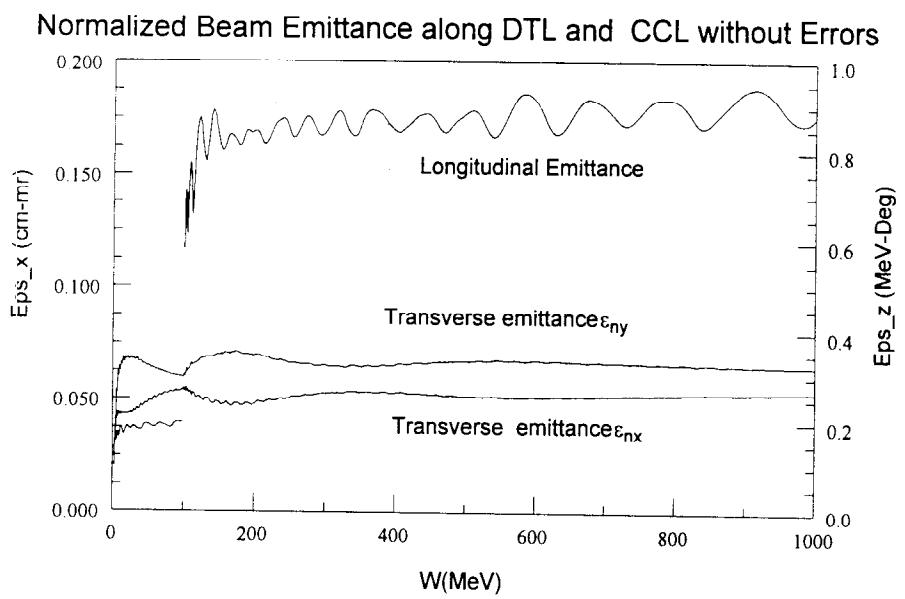

Fig. 8. The normalized rms emittances in the DTL and CCL without longitudinal and transverse linac errors.

Figure 8 shows the normalized rms emittances in the DTL and CCL. The simulation was performed with using the beam particle distribution at the exit of MEBT. The discontinuity of longitudinal emittance is caused by the jump in the frequency from 402.5 MHz to 1207.5 MHz.

(B) The beam dynamics calculation including Transverse and Longitudinal Errors.

The longitudinal errors consist of rf amplitude and rf phase errors. These errors are caused by the errors from the Klystron output phase and amplitudes. The power partitioning of linac divides the linac into multiple modules. Each module, which is powered by one or more Klystrons, contains a number of segments. To perform longitudinal dynamics calculations including errors, we then assume the same values of phase and amplitude errors at each module. According to the linac partitioning performed by James Billen, the CCL is 433m long and the total copper power consumed is 62.68 MW in the CCL. A total 52 of Klystrons (2MW per Klystron) are required in the CCL.

To study the longitudinal errors in the CCL, we performed several scenarios: ±0.5% rf amplitude error and ±0.5° rf phase error, ±0.25% rf amplitude error and ±0.5° rf phase error±0.8%, rf amplitude error and ±0.8° rf phase error. In the following figures 9,10,and 11, we assumed the phase and amplitude errors only in the CCL. Also the particle distribution at the entry to the DTL is created that represents the beam ellipse parameters after the MEBT. These figures show that the longitudinal errors generally do not cause transverse mismatch or envelope oscillations. But, as is observed, the energy oscillation persists through the linac. This reflects the synchrotron motion of beam bunch in the separatrix.

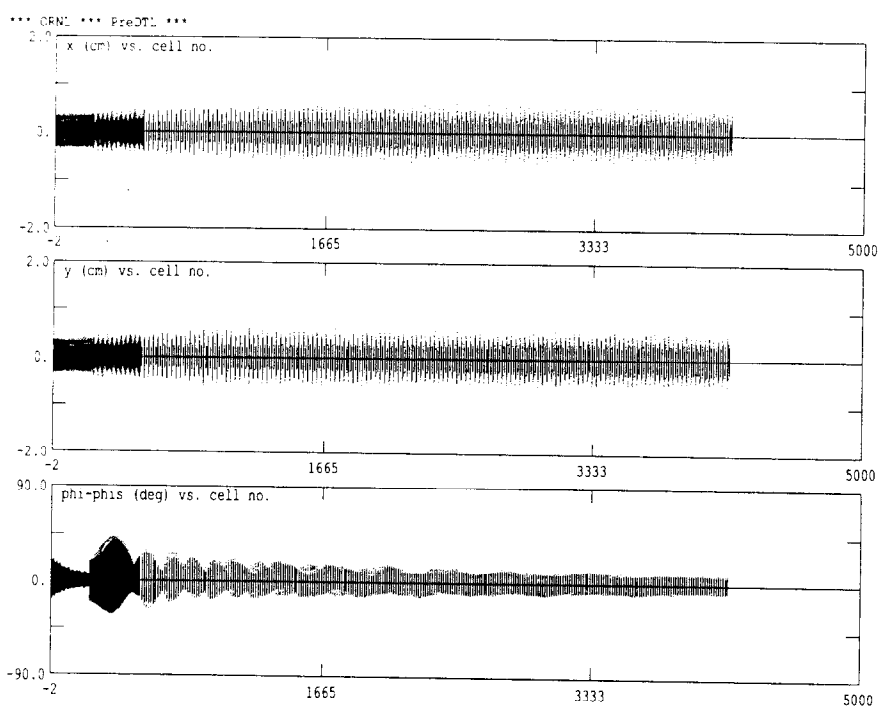

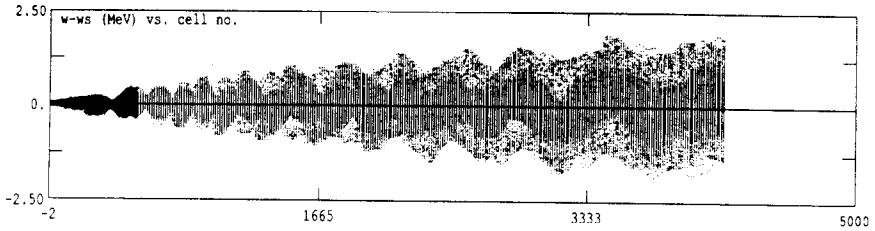

Fig. 9. Beam profiles along linac at ±0.5% RF Amplitude error, ±0.5 Deg. phase error in CCL

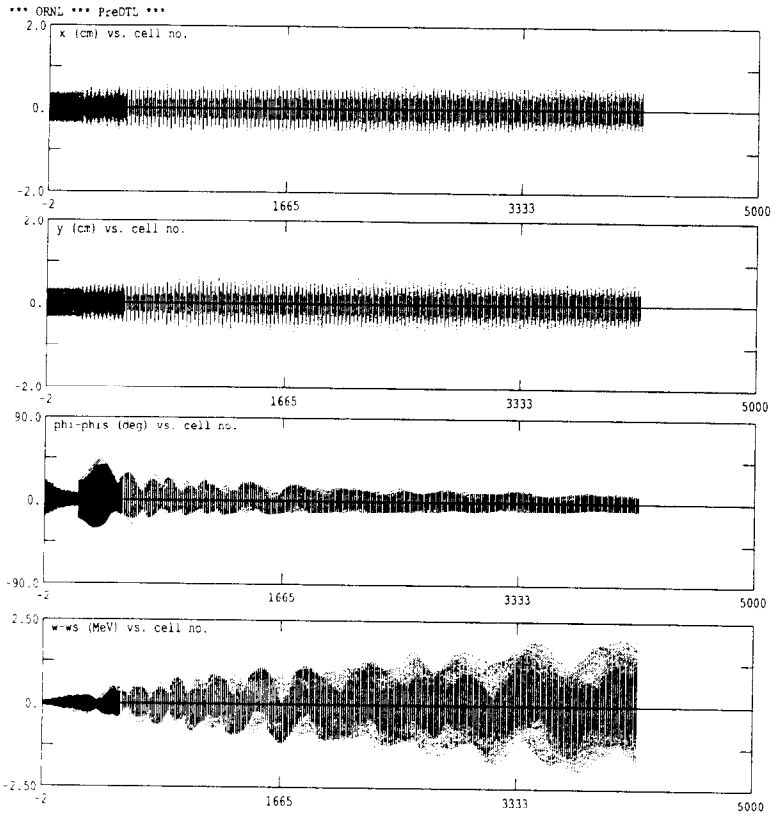

Fig. 10. Beam profiles along linac at ±0.25% RF Amplitude error, ±0.5 Deg. phase error in CCL

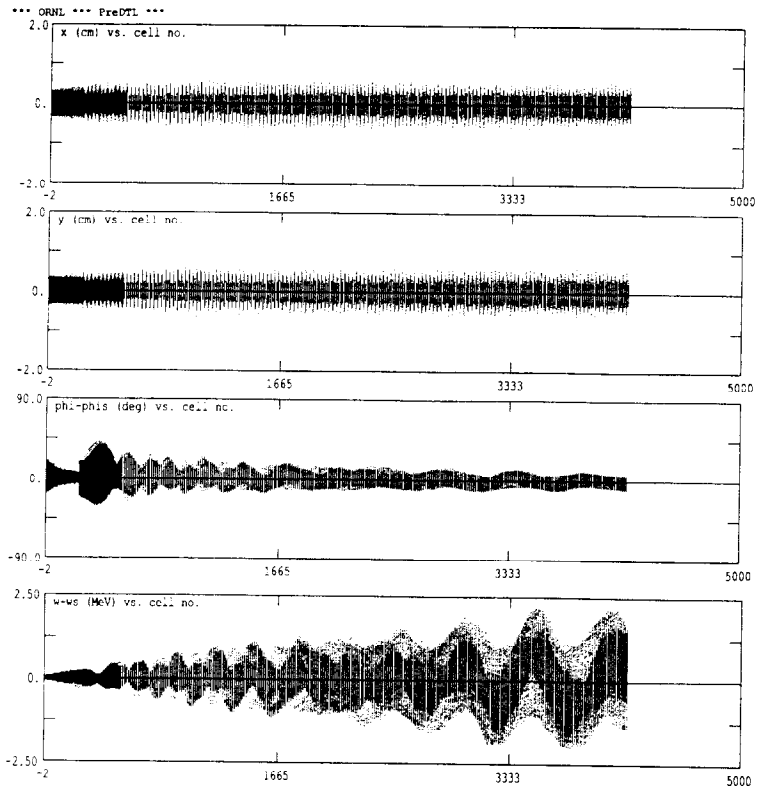

Fig. 11. ±0.8% RF Amplitude error, ±0.8Deg. phase error in CCL

In studying the transverse quadrupole errors, we included the following error items shown in Table 1 and Table 2.:

Table 1. Error limits for components of DTL

description of error	limit on error
quadrupole transverse displacement	5 mil
quadrupole tilt	0.29°
quadrupole roll	0.25°
quadrupole gradient error	0.25%

Table 2. Error limits for components of CCL

description of error	limit on error
quadrupole transverse displacement	5 mil
quadrupole tilt	0.29°
quadrupole roll	0.25°
quadrupole gradient error	0.25%
module field amplitude error(dynamic)	0.25%
module phase error(dynamic)	0.5°

In Fig 12, we present beam profiles along the linac resulting from both transverse and longitudinal errors for both DTL and CCL. The particle distribution is raw distribution after transported the MEBT instead of matched beam at the entrance to the DTL. Instead

of performing numerous simulation runs to survey the statistical features, we show one simulation run to show the characteristics of the errors along the linac in this study.

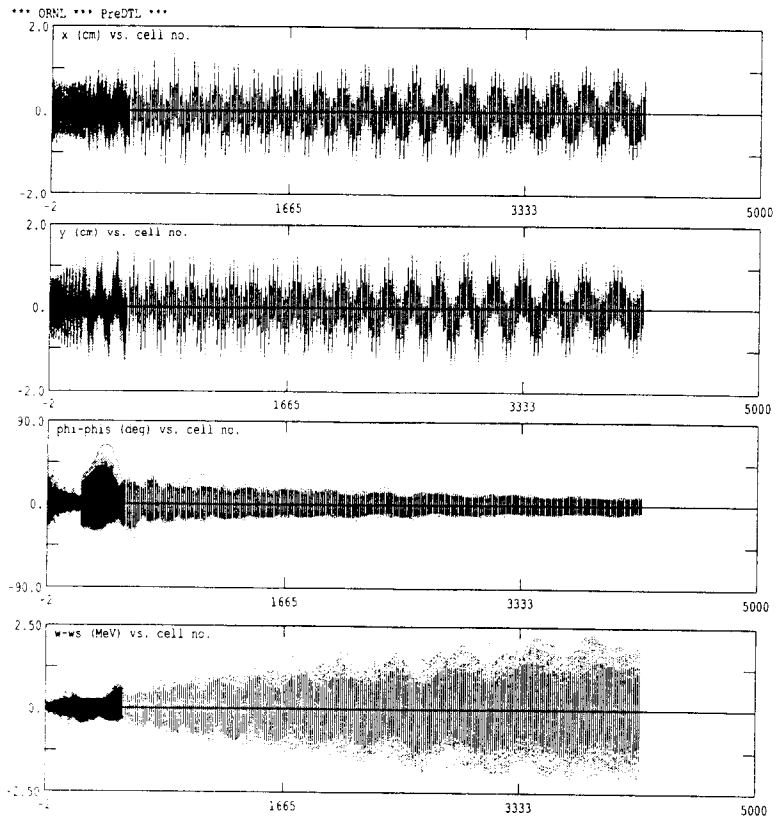

Fig 12. Beam profile along linac with both Quadrupole misalignment, gradient errors and rf module amplitude phase errors are included in the simulations ($\delta A=\pm 0.25\%$, $\delta\phi=\pm 0.5°$).

The maximum and minimum beam x radii and the rms beam x radii are shown in Figure 13 along the linac. Knowing that the longitudinal errors did not modify the transverse dimensions, the beam size in the CCL could be larger than the bore radius 1.5 cm. Therefore, some fraction of beam will be lost in the CCL with the assumed quadrupole errors.

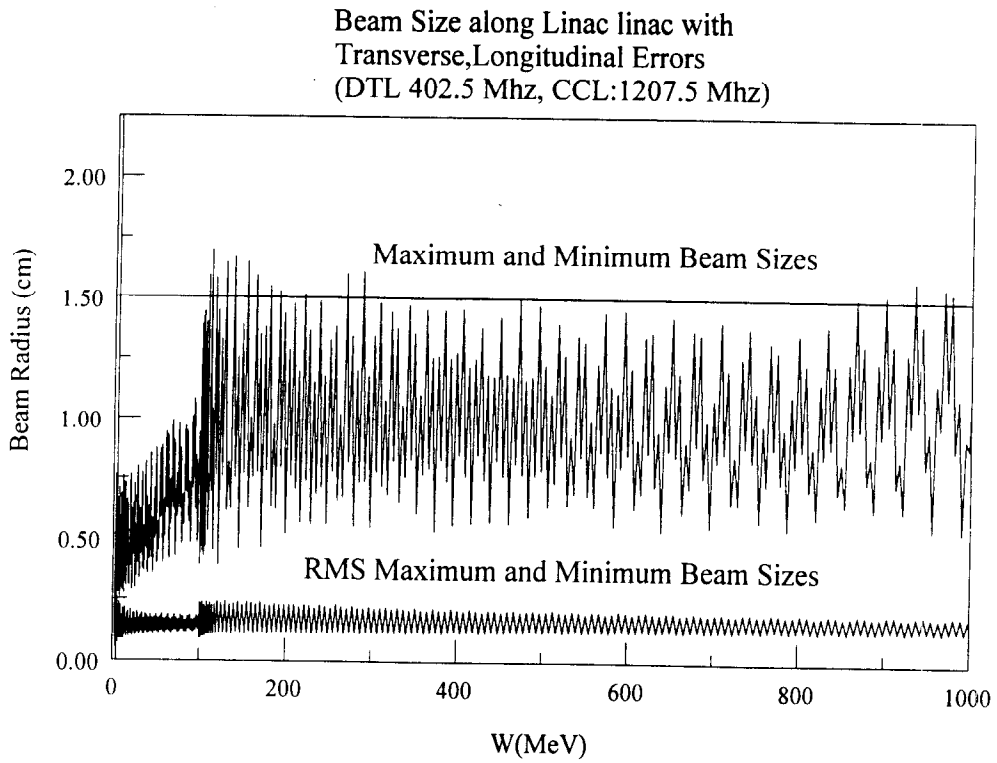

Fig. 13 The Maximum and Minimum Beam x sizes and RMS beam x sizes along the linac. The rf amplitude errors, phase errors in DTL, and CCL in addition to the transverse quadrupole errors are included.

The normalized rms beam emittances along the linac are shown in Figure 14. Again, the longitudinal emittance jump is a result of artifact of frequency tripling effect.

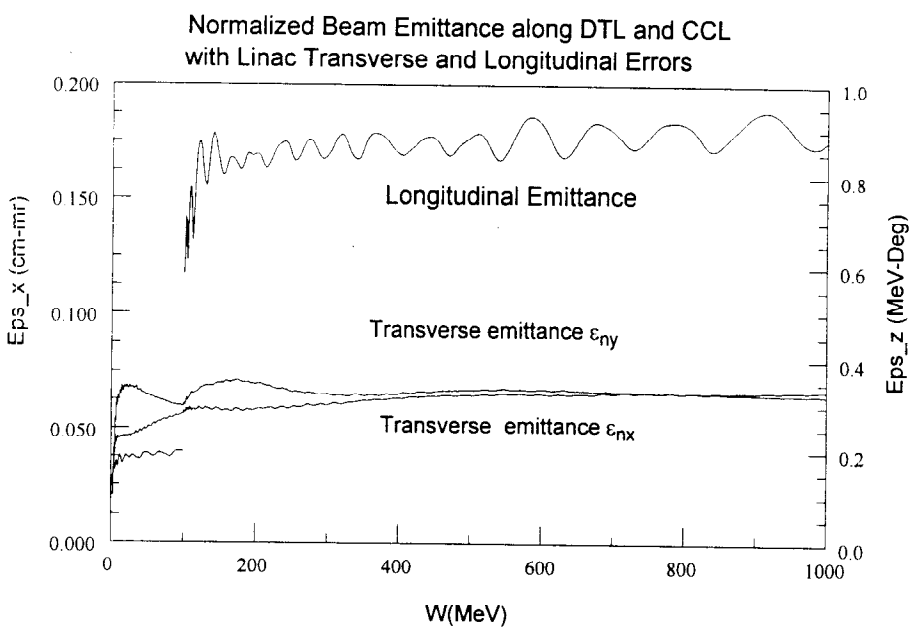

Fig. 14 The normalized beam emittances along the DTL and CCL including the Transverse and Longitudinal linac errors.